Plasma Physics and
Controlled Fusion

PURPOSE-LED
PUBLISHING™

PAPER • OPEN ACCESS

Self-consistent modeling of STEP flat top scenario with realistic electron cyclotron heating and current drive

To cite this article: R Sharma *et al* 2026 *Plasma Phys. Control. Fusion* **68** 015011

View the article online for updates and enhancements.

You may also like

- Edge fluctuation measurements in EDA H-mode and QCE plasmas in ASDEX Upgrade using the correlation electron cyclotron emission diagnostic
J Schellpfeffer, B Vanovac, M Faitsch et al.
- Localizing C III emission using multi-delay coherence imaging spectroscopy on W7-X
N Lonigro, D M Kriete, V Perseo et al.
- Investigation of the fast ion driven kinetic ballooning mode in FIRE mode discharge through gyrokinetic simulations
D Kim, B J Kang, S J Park et al.

This content was downloaded from IP address 194.81.223.66 on 16/01/2026 at 11:43

IOP Publishing Plasma Phys. Control. Fusion 68 (2026) 015011 https://doi.org/10.1088/1361-6587/ae2a6b

Plasma Physics and Controlled Fusion

Check for updates

OPEN ACCESS

RECEIVED
13 August 2025

REVISED
26 November 2025

ACCEPTED FOR PUBLICATION
9 December 2025

PUBLISHED
5 January 2026

Original content from this work may be used under the terms of the Creative Commons Attribution 4.0 licence.

Any further distribution of this work must maintain attribution to the author(s) and the title of the work, journal citation and DOI.

PAPER

Self-consistent modeling of STEP flat top scenario with realistic electron cyclotron heating and current drive

R Sharma[1,*], K Kirov[1], S Freethy[1], D Brunetti[1], F J Casson[1], F Eriksson[1], L Figini[3], M Henderson[2], S Marsden[1], H Meyer[2], Ž Stancar[1], E Tholerus[1], T Wilson[1] and STEP team[4]

[1] UKAEA (United Kingdom Atomic Energy Authority), Culham Campus, Abingdon, Oxfordshire OX14 3DB, United Kingdom
[2] UKIFS (UK Industrial Fusion Solutions Ltd.), Culham Campus, Abingdon, Oxfordshire OX14 3DB, United Kingdom
[3] Istituto per la Scienza e Tecnologia dei Plasmi, Consiglio Nazionale delle Ricerche, 20125 Milano, Italy
[4] See Slide 3 of https://conferences.iaea.org/event/392/contributions/35746/attachments/19773/36941/2_Meyer_IAEA_FEC_2025.pdf.
[*] Author to whom any correspondence should be addressed.

E-mail: ridhima.sharma@ukaea.uk

Keywords: ECCD, STEP, self-consistent modeling

Supplementary material for this article is available online

Abstract

The spherical tokamak for energy production (STEP) is the UK's flagship program to design a prototype fusion power plant capable of delivering net electricity to the grid. Due to geometric constraints in spherical tokamaks, STEP is being developed for fully non-inductive operation, relying primarily on microwave-based electron cyclotron (EC) and electron Bernstein wave systems for plasma heating and current drive (HCD). A key requirement for achieving this operation is the optimization of these systems to ensure high wall-plug efficiency and reliable current profile control. This paper presents a self-consistent modeling approach using the JINTRAC framework, where the JETTO transport code is coupled with the GRAY quasi-optical beam-tracing code. Previous scenario development relied on simplified, prescribed EC current drive (ECCD) profiles. In this work, these were replaced with the profiles derived from detailed parametric GRAY scans, optimized for launcher geometry, frequency, and polarization. These realistic ECCD profiles are integrated into a fully self-consistent JETTO/GRAY simulation, capturing the dynamic interplay between plasma transport, heating, and current evolution. The methodology developed in this study offers a more accurate representation of HCD dynamics and is applicable to future STEP scenario development.

1. Introduction

The spherical tokamak for energy production (STEP) is the United Kingdom's program to design and construct a prototype fusion power plant that delivers net electricity to the grid. In conventional tokamak designs, the central solenoid plays a crucial role in generating the plasma current during the ramp-up and steady-state phases. However, due to the compact nature of spherical tokamaks, space constraints significantly limit the size and effectiveness of the central solenoid, making it inadequate for sustaining the required plasma current. As a result, STEP is being designed for fully non-inductive operation throughout the steady-state (flat-top) phase and for a significant portion of the ramp-up phase.

To achieve this, STEP will utilize a microwave-based heating and current drive (HCD) system, integrating electron cyclotron (EC) and electron Bernstein waves as the primary means of plasma HCD. This decision is based on a thorough evaluation of HCD technologies, considering efficiency, current drive capability, compatibility, cost, maintenance, structural impact, and technological readiness [1]. Optimizing the HCD system is crucial, as it represents one of the largest consumers of internal power in a fusion power plant [2]. Improving its wall-plug efficiency is essential for achieving net electricity output and ensuring sustainable and economically viable fusion energy production.

© 2026 Crown copyright, United Kingdom Atomic Energy Authority (UKAEA)

A key aspect of STEP's scenario development is the self-consistent modeling of plasma transport, heating, and current drive. This is achieved using the JINTRAC suite of codes [3], which offers a comprehensive framework for simulating plasma equilibrium, transport, and heating in fusion devices. Within JINTRAC, the JETTO transport code is coupled with a quasi-optical beam-tracing code GRAY [4], enabling a self-consistent representation of EC heating effects and current drive efficiency by integrating transport and wave propagation calculations.

Until now, flat-top modeling and scenario design have been conducted using a prescribed EC and current drive (ECCD) profile derived from an analytic formula that accounts for temperature and density dependencies. In this work, we aim to replace the prescribed ECCD profile with a more realistic one and perform a fully self-consistent simulation to capture the dynamic interaction between the plasma and ECCD.

First, GRAY is run in standalone mode using the magnetic equilibrium and kinetic profiles from the steady-state scenario. For each launcher position, a parametric scan is performed across frequency, toroidal and poloidal launch angles, and polarization (O-mode or X-mode), generating a dataset of ECCD efficiency and corresponding current profile shapes. From this dataset, the optimal launch conditions are selected to best match the target current drive profile. These serve as the starting point for a JETTO simulation using GRAY, which self-consistently computes the EC HCD in response to the evolving plasma profiles.

This study focuses on achieving fully self-consistent scenario modeling with realistic HCD. To accomplish this, an iterative optimization process is performed, including:

1. Determining the optimal launching parameters to achieve the desired HCD profiles.
2. Evaluating the time evolution of the coupled JETTO/GRAY simulation and comparing it with the steady-state reference case, in order to confirm that the self-consistent solution does not deviate significantly from the simplified prescribed-ECCD scenario.

By integrating JETTO with the GRAY EC launch conditions within JINTRAC, this study provides a more precise and self-consistent representation of HCD dynamics in STEP. It evaluates the feasibility of steady-state operation using EC launchers by analyzing their direct impact on plasma parameters. Additionally, this methodology can be extended to future STEP prototype designs.

2. Selecting EC launching condition for STEP steady-state phase

For STEP scenario modeling, JINTRAC—specifically the JETTO transport code, coupled with supporting modules—has been used to obtain a steady-state simulation for the preliminary STEP prototype power plant. JINTRAC is an integrated framework of tokamak-physics codes that enables self-consistent modeling of plasma equilibrium, transport, heating, and current drive across different operational phases [3]. The details of the flat-top operational space for the STEP Prototype Plant (SPP1 EC-HD) are provided in [5], which is based on a simple transport model. The reference flat-top plasma used in this paper is also based on [5], but it includes interpretive impurity treatment and is designed to achieve a steady state using a predefined EC HCD profile. This profile is derived from an analytic formula that accounts for temperature (T_e) and density (n_e) dependencies—referred to as prescribed current drive. In JETTO, this is implemented via a scaling parameter called ECCDNORM, and the EC-driven current density at a given radius ρ, $J(\rho)$, is defined as:

$$J(\rho)\left[\mathrm{kA.m^{-2}}\right] = \mathrm{ECCDNORM} \times \frac{T_e\,[\mathrm{keV}]}{n_e\left[10^{19}\mathrm{m^{-3}}\right]} \times \bar{Q}(\rho) \times P_{\mathrm{EC}}\,[\mathrm{MW}]$$

where, P_{EC} is the EC power, $\bar{Q}(\rho)$ is the normalized EC power density profile, given by:

$$\bar{Q}(\rho) = \frac{Q(\rho)}{\int_0^{\rho_{\mathrm{sep}}} 2\pi\rho' Q(\rho')\,d\rho'}.$$

The resulting plasma profiles—including temperature, density, safety factor, and current density contributions—for the SPP1 EC-HD case are shown in figure 1. The EC heating and CD derived following this recipe are referred to as reference case in this paper.

The reference profiles shown in figure 1 are based on the flat-top operating points derived in Tholerus *et al* [5]. These equilibria were selected after parameter scans in normalized β, Greenwald fraction, auxiliary power, and radiation constraints, and represent the best-performing non-inductive steady-states under STEP design assumptions. In their modeling, JETTO uses prescribed transport coefficients

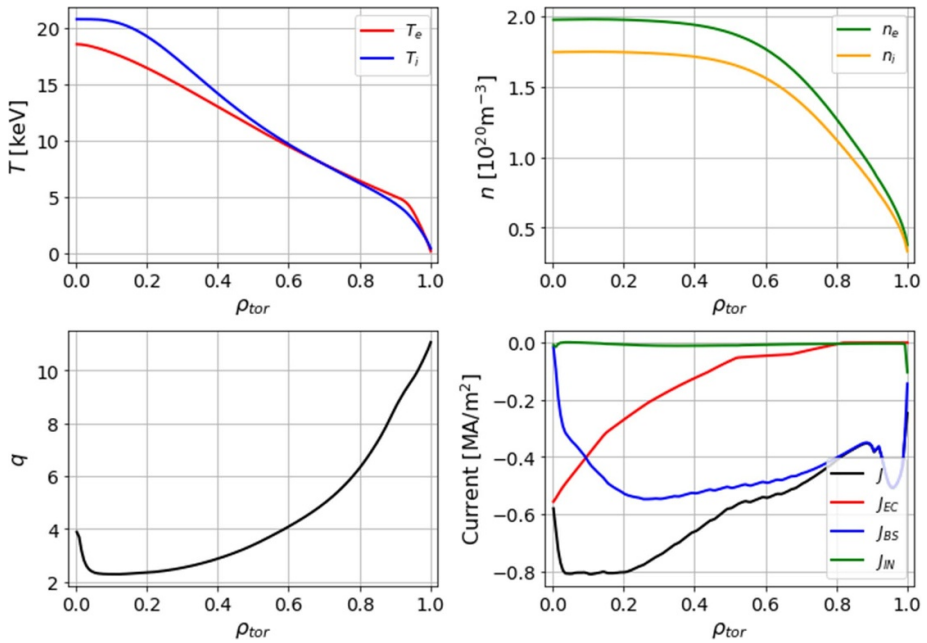

Figure 1. Plasma profiles for the STEP fully non-inductive steady-state scenario with EC heating and current drive (SPP1 EC-HD). The top plots show electron and ion temperature (left) and density (right), while the bottom plots display the safety factor (q) profile (left) and total current density (J) and its contribution from EC (J_{EC}), bootstrap (J_{BS}) and inductive current (J_{IN}) (right).

that are globally rescaled to match the target β while preserving electron-to-ion diffusivity ratios guided by gyrokinetic modeling. Pellet fuelling is included as a continuous source, and the fuelling rate is adapted to reach a target Greenwald density fraction.

The methodology to replace the prescribed current drive profile with a realistic ECCD profile involves performing parametric scans using the GRAY code. GRAY is a beam-tracing code developed to simulate EC wave propagation, absorption, and current drive in tokamak plasmas [6]. It uses a complex eikonal method to model Gaussian beam propagation and accounts for diffraction effects, incorporating a cold propagation model with a fully relativistic damping model for wave propagation and current drive. For current drive calculations, the code incorporates response functions in the linear adjoint model [7], which include trapped-particle effects and corrections to the parallel conductivity. In its single-ray mode, GRAY utilizes the linear adjoint approach to calculate current drive efficiency [8]. Subsequent enhancements have introduced momentum-conserving collision corrections, further improving the precision of the current drive calculations [9]. This enables precise modeling of power absorption and current drive. GRAY can operate as a standalone tool or be integrated with the plasma transport code JETTO for self-consistent transport simulations within the JINTRAC suite.

Extensive ray-tracing scans were carried out using the standalone version of GRAY to determine optimal launcher configurations and operating parameters for efficient ECCD. These scans explored a full range of launching conditions, including poloidal and toroidal angles and wave frequencies, for both O-mode and X-mode waves (figure 2, left). The analysis was performed for a selected set of EC launchers (figure 2, right), based on steady-state equilibrium and plasma profiles, with conditions taken from the steady-state JETTO simulation at 200 s (figure 1). For each combination of injection angle and frequency, single-ray simulations were run to evaluate the resulting ECCD profiles. The parameters thus optimized—frequency, toroidal and poloidal angles, and input power—were then integrated into JETTO for self-consistent plasma transport modeling. A summary of the scanned parameter space is provided in figure 2, along with the radial and vertical positions of the launchers used in this study. It should be noted that, as the STEP design continues to evolve, these launcher parameters are expected to change in future iterations of the modeling.

Figure 3 illustrates the efficiency (η) in A/W, defined as the ratio of EC-driven current (I_{EC}) to the injected EC power (P_{EC}), for each launcher across the scanned frequency range for O-mode. Each dot in the figure corresponds to the outcome of a single GRAY run from the parametric scans, representing the current driven per watt of absorbed EC power for a specific combination of frequency, poloidal angle, and toroidal angle (see figure 2, left). The vertical axis therefore shows $\eta = I_{EC}/P_{EC}$ (A/W), while the horizontal axis indicates the corresponding radial deposition location, ρ. The dot color indicates

Parameter	Range	Increment
Frequency	60–240 GHz	5 GHz
Toroidal Angle	-35° to +5°	5°
Poloidal Angle	Determined by launcher access	2.5°

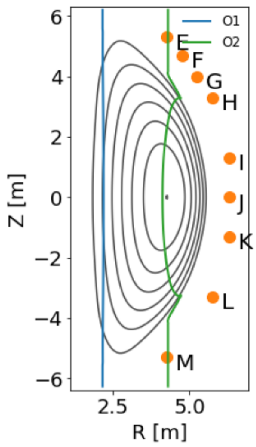

LP	R (cm)	Z (cm)
E	425.0	530.0
F	475.0	470.0
G	525.0	400.0
H	575.0	330.0
I	630.0	130.0
J	630.0	0.0
K	630.0	-130.0
L	575.0	-330.0
M	425.0	-530.0

Figure 2. Parameter table (left) showing the scan ranges and increments for frequency, toroidal, and poloidal launch angles. The central panel shows the poloidal view of the plasma cross-section with the EC launcher positions (LP) indicated. The table on the right lists the corresponding radial (R) and vertical (Z) coordinates of each launcher. The fundamental (O1) and second harmonic (O2) cold resonance layers for 150 GHz are also plotted on the poloidal cross-section to illustrate the expected absorption regions.

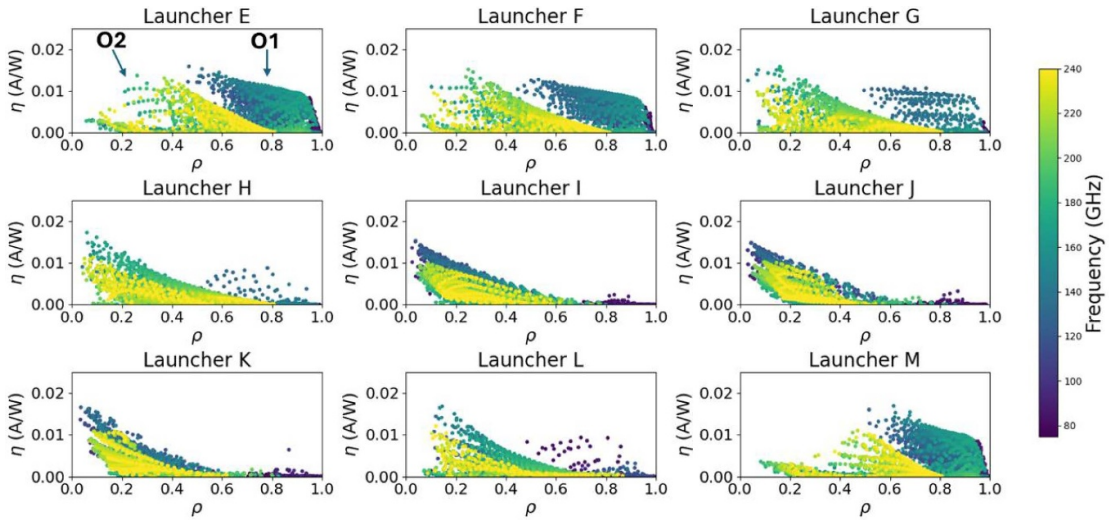

Figure 3. EC efficiency ($\eta = I_{EC}/P_{EC}$) over angle scans for the range of frequencies for all launchers for O mode launch. Each dot corresponds to η obtained from a single GRAY run with a distinct combination of frequency, poloidal angle, and toroidal angle (see scan ranges in figure 2, left). Only cases with full EC power absorption are included. Dot color indicates the launch frequency (60–240 GHz), distinguishing between fundamental (O1, lower-frequency/blue) and second harmonic (O2, higher-frequency/green) absorption. Groups of points corresponding to the O1 and O2 launchers are marked by arrows in the first plot in (a).

the launch frequency, ranging from 60 GHz (blue) to 240 GHz (green), which also reflects whether the absorption occurs at the fundamental (O1) or second harmonic (O2). The scatter therefore maps how current drive efficiency depends simultaneously on frequency, harmonic, and injection geometry.

The scans guided the selection of the optimal launcher configurations for each radial region. Equivalent scans were also performed for X-mode; however, the O-mode configuration demonstrated superior efficiency and accessibility under core-access conditions due to reduced accessibility limitations and favorable resonance behavior. It also aligns with the ECCD profile requirements set for STEP, where current drive is needed primarily in the central region ($\rho \lesssim 0.5$) [2].

To obtain the most efficient set of launching conditions, launcher configurations were first screened based on their current drive efficiency, and only those with the highest efficiency were retained. From this subset, a combination of 14 launchers and corresponding power levels was selected to best match

LP	f (GHz)	R (m)	Z (m)	Pol. (deg)	Tor. (deg)	P (MW)
E1	210	4.25	5.30	65	-25	36
E2	135	4.25	5.30	57	-25	4.9
E3	215	4.25	5.30	65	-25	4.3
E4	145	4.25	5.30	60	-20	6
E5	140	4.25	5.30	55	-25	10
F1	185	4.75	4.70	60	-25	31.2
G1	160	5.25	4.00	55	-20	4
H1	165	5.75	3.30	45	-25	6
L1	170	5.75	-3.30	-42.5	-25	40
M2	150	4.25	-5.30	-50	-25	8.6
M3	160	4.25	-5.30	-47	-25	6.2
M4	160	4.25	-5.30	-45	-25	2.9
M5	160	4.25	-5.30	-47	-20	2.1
M6	160	4.25	-5.30	-40	-20	0.8

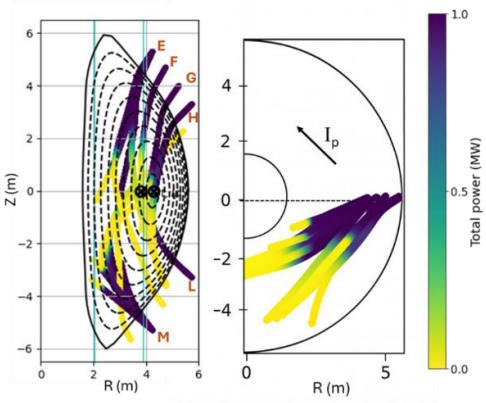

Figure 4. (Left) table of selected EC launchers (LP) used in the self-consistent JETTO/GRAY simulation, including their radial (R) and vertical (Z) positions, poloidal and toroidal launch angles, frequency, and allocated power. These launchers were chosen based on the parametric efficiency scans shown in figure 3. (Right) poloidal and toroidal views of the corresponding beam trajectories inside the plasma. The beam color indicates the remaining EC power along the trajectory, from purple (full input power at the launcher) to yellow (zero power after absorption), thereby illustrating the power deposition location for each beam in the plasma.

the target ECCD-driven current and heating profiles, while also ensuring that the total driven current was consistent with the reference run.

The GRAY code was then re-run for these selected launchers, with the beam waist set to 6 cm at the launcher aperture. To obtain the EC power in each launcher, the total power and current drive profiles from GRAY were linearly scaled to match the reference steady-state case. The optimized launching conditions (power, launching angles, and frequency) obtained from stand-alone GRAY scans (presented in figure 4) are used as inputs for the plasma transport code JETTO, as described in the next section. In figure 4, the left table summarizes the selected launcher positions and parameters, while the right panel shows the corresponding beam trajectories with a color map of the absorbed power. This illustrates how the chosen set of launchers delivers power and current drive across the plasma volume.

3. JETTO/GRAY coupled self-consistent modeling

In the preceding section, a solution for launcher configurations designed to match the prescribed ECCD profiles used in the reference steady-state simulation [5] was presented. This section discusses the results of the self-consistent modeling obtained by replacing the prescribed ECCD with a realistic profile. The outcomes of this fully integrated simulation, where the plasma evolves with a realistic ECCD over a 50 s period, are presented below.

Figure 5 illustrates the flow diagram of the JINTRAC suite of codes employed for modeling the plasma during the STEP flat-top phase, as previously described in section 2 and referenced in [5]. In this diagram, the JETTO transport code serves as the central component of the modeling framework. JETTO receives inputs from various modules, including the equilibrium solver, impurity transport code (SANCO), and heating models. It applies boundary constraints based on the selected transport model and updates plasma profiles, which are then fed back into the relevant modules. This iterative process continues for each time step or equilibrium adjustment.

For this work, the key feature of the integrated approach is the coupling of the GRAY code within the heating module for EC heating. For the self-consistent simulation, JETTO is coupled with GRAY, enabling JETTO to invoke the GRAY subroutine at user-defined intervals or whenever there is a change in plasma profiles or equilibrium conditions. This integration ensures that the EC HCD profiles are dynamically updated in response to the evolving plasma state, enabling self-consistent plasma evolution. This methodology provides a more accurate representation of plasma behavior during the STEP flat-top phase and offers insights into the performance and optimization of the STEP prototype powerplant. The following section discusses the results from the self-consistent run, where the prescribed current drive is replaced with a realistic ECCD.

3.1. Self-consistent evolution of plasma profiles using JETTO/GRAY coupling

Figure 6 presents the results from the completed self-consistent run for 1 s. The reference run, with prescribed ECCD and heating profiles, evolved up to 200 s, which is taken as the nominal end of the

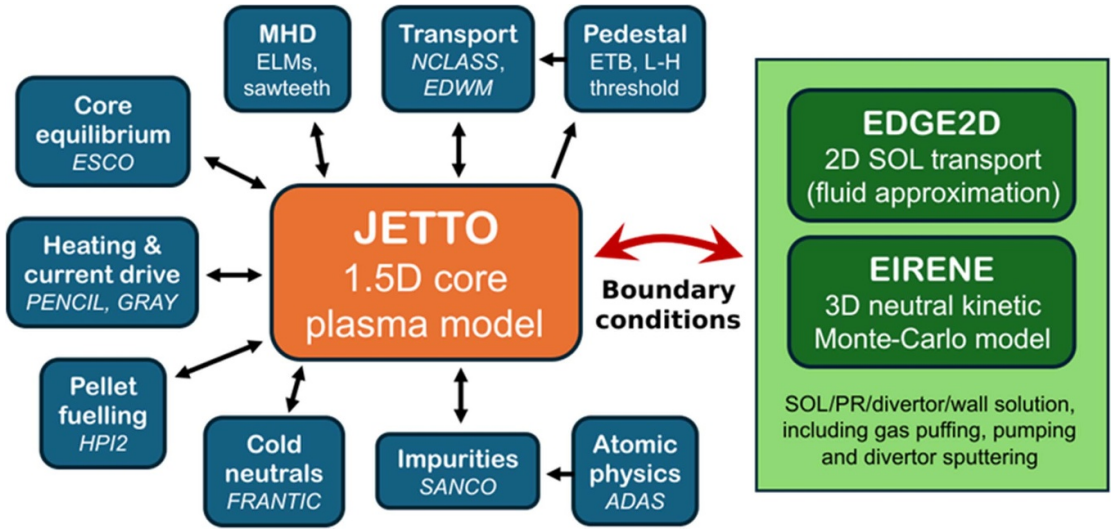

Figure 5. Flowchart of JINTRAC modeling suite.

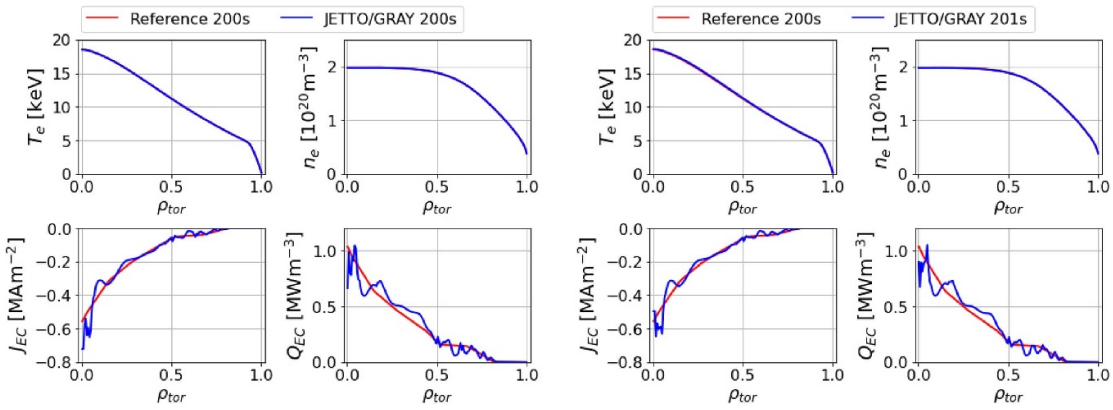

Figure 6. Plasma quantities at the 200 s (left) and at 201 s (right) for the self-consistent JETTO/GRAY coupled self-consistent simulation (blue) compared with the reference scenario (red). The time 200 s corresponds to the nominal end of the steady-state flat-top phase in the reference scenario.

steady-state phase. Immediately following, the prescribed HCD profile is replaced with the HCD profiles obtained from 14 EC beam launchers optimized in section 2 (figure 4). On the left side, profiles for electron temperature (T_e), density (n_e), EC current density (J_{EC}), and EC heating density (Q_{EC}) at 200 s are displayed. The density and temperature profiles are exactly overlapping between the reference (red) and JETTO/GRAY coupled self-consistent simulation (blue) cases. Similarly, a good agreement is observed in the J_{EC} and Q_{EC} profiles. The figure on the right includes the evolution of the same plasma parameters after 1 s of the JETTO/GRAY coupled self-consistent simulation. Only nominal changes are observed in the temperature and density profiles; and the EC HCD profile shows no significant deviation after 1 s. However, it should be noted that the simple transport models used in the modeling do not have strong sensitivity to the current profile. In both the reference and self-consistent cases, radial transport is modeled in JETTO using prescribed transport coefficients that are globally adjusted to reproduce the target normalized β, with electron-to-ion diffusivity ratios guided by gyrokinetic modeling [5]. Particle fuelling is represented by a continuous pellet source with density feedback control, consistent with the STEP flat-top scenario in [5], and is the primary mechanism for maintaining the density profile during the flat-top phase.

The differences between the reference and self-consistent cases are due to the different representations of the ECCD profile. In the reference case, the profile is prescribed analytically and scaled smoothly, whereas in the JETTO/GRAY case it is constructed from 14 discrete launcher beams with finite widths. This produces localized peaks in the EC heating and current density profiles, which appear less smooth but are physically realistic. Despite these localized variations, plasma equilibrium remains fully

consistent, as JETTO evolves the total current balance self-consistently. The bootstrap and inductive current components adjust to compensate for the localized ECCD structures, preserving Ampere's law and maintaining a stable overall q profile (see section 3.2).

In the reference steady-state simulation, the current diffusion rate or resistivity was increased by a factor of 27. However, in the JETTO/GRAY self-consistent simulation with a realistic current drive, this scaling was removed to accurately capture a realistic relationship between heating and current diffusion dynamics. Since the impact of EC beams on electron temperature occurs on a very short timescale within the JETTO/GRAY model, it is important to maintain a physically accurate current diffusivity to realistically capture the beam-plasma interactions.

Once consistency was confirmed in the first second of the simulation (figure 6), the self-consistent simulations were extended beyond the reference run at 200 s. The simulations were conducted with successive endpoints at 205 s, 220 s, 235 s, and 250 s, using the final state of each run as the starting condition for the next. This step-by-step approach allowed the plasma evolution to be tracked over 50 s, with key plasma parameters observed at each stage.

Figure 7(a), similar to the previous figure, presents the evolution of plasma profiles, including temperature, density, EC heating, and driven current over time. The results indicate strong consistency across all runs, with density and electron temperature profiles remaining nearly identical throughout. Additionally, the current density and power deposition profiles show minimal deviation from the initial ECCD and heating deposition, confirming the robustness of the self-consistent simulation and approach toward steady state.

To quantify these differences, figure 7(b) shows the absolute error between each self-consistent run (205 s, 220 s, 235 s, 250 s) and the reference case at 200 s for both J_{EC} and Q_{EC}. The errors remain small and localized, confirming that the deviations from the prescribed steady state are minor and that the solution converges consistently toward a new equilibrium.

3.2. Current contribution evolution

Figure 8 shows the total current density (J) and its contributions from bootstrap (J_{BS}), EC (J_{EC}), and inductive (J_{IN}) contributions for the self-consistent modeling at different time intervals, compared to the reference steady-state run. The reference case shown in red has been modeled for a long enough period of up to 200 s with prescribed EC power deposition and current drive. Plasma equilibrium and kinetic profiles at 200 s are then used as a target scenario in which prescribed EC heating and CD is replaced with self-consistent profiles provided by JETTO/GRAY. The resulting current density contributions at 5 s (blue), 20 s (green), 35 s (brown) and 50 s (orange) are shown for comparison in figure 8. The results indicate that while the total current density in the self-consistent simulations generally follows the reference case, discrepancies in the core region ($\rho < 0.2$) arise due to challenges in matching the EC current density (J_{EC}) exactly due to very small plasma volume. On the other hand, the bootstrap current density (J_{BS}) remains closely aligned across all runs as there is no significant deviation in plasma pressure profiles.

The inductive current density (J_{IN}) arises due to discrepancies between the externally driven ECCD (J_{EC}), as provided by the JETTO/GRAY simulations, and the prescribed reference current profile. When the prescribed ECCD is replaced with a self-consistent profile that does not perfectly match the reference, a back electromotive force (EMF) (E_{EMF}) is generated in accordance with Faraday's law. This induced electric field acts to counter the difference and redistributes current throughout the plasma. In modeling this process, the resulting E_{EMF} drives an inductive current according to Ohm's law, $E_{EMF} = \eta J_{IN}$, where η is plasma parallel resistivity.

Since resistivity depends strongly on electron temperature, $\eta \sim T_e^{-3/2}$, the same electric field induces much larger J_{IN} in the core than at the edge. As a result, the total current density, $J = J_{IN} + J_{EC} + J_{BS}$, begins to evolve in response to this inductive contribution. The rate of this evolution is governed by the current diffusion time, $\tau = \mu_0 a^2/\eta$, with a being the minor radius, which is on the order of a few thousand seconds in the core and a few tens of seconds at the edge. Consequently, J in the core evolves very slowly, of the order of thousands of seconds, while J in plasma periphery changes almost instantly within a few seconds. Therefore, it will be very challenging in our simulations to match perfectly the reference J (and q) with JETTO/GRAY ECCD over the whole plasma cross-section.

Because temperature influences both resistivity and the efficiency of current drive, even small variations in the ECCD profile can significantly affect the current distribution. Therefore, precise matching of the ECCD profile from the GRAY scans to the prescribed target is essential—not only to accurately reproduce the desired current distribution, but also to minimize the generation of compensatory inductive currents. As shown in figure 8 (at 5 s), initial mismatches in the ECCD profile led to a noticeable

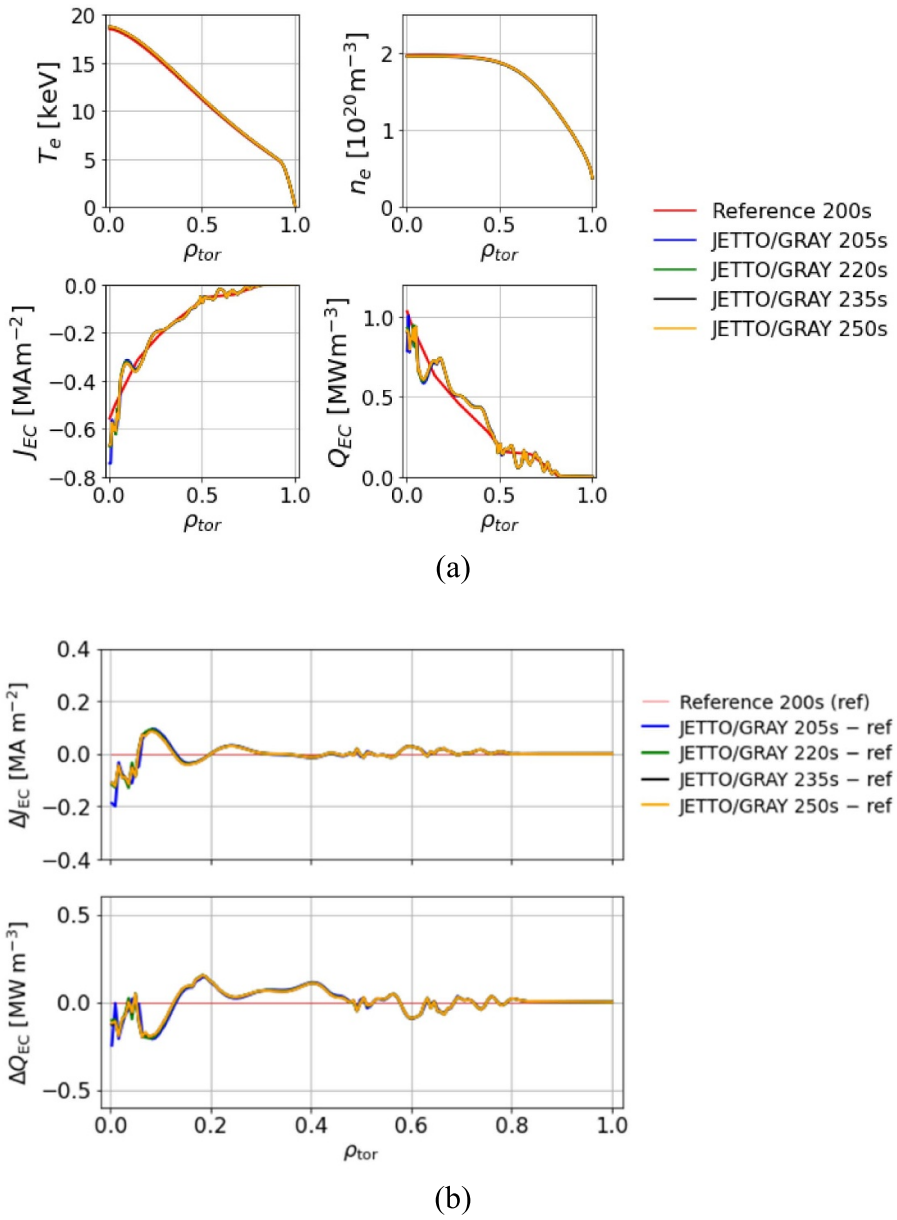

Figure 7. (a) Electron temperature, density, EC current density and power deposition profiles for the end time-slice of reference and for the self-consistent simulations. (b) Absolute error of the EC-driven current density (ΔJ_{EC}) and power deposition (ΔQ_{EC}) relative to the reference case at 200 s.

E_{EMF} and the generation of J_{IN}, which gradually subsides as the plasma evolves and the current profile adjusts to restore balance.

Figure 9 illustrates the radial profiles of integral quantities within the flux surface such as, total current (I_{total}), EC-driven current (I_{EC}), and injected EC power, (P_{EC}) for the self-consistent simulations at the end of each run. The total current profile shows excellent agreement with the reference steady-state case. In the modeling, the injected EC power is set to approximately 150 MW in the reference run and 160 MW in the self-consistent JETTO-GRAY simulations. The I_{EC} profile in the JETTO-GRAY case is slightly reduced beyond $\rho = 0.6$, attributed to marginally lower ECCD efficiency in combination with the larger plasma volume. As a result, the global current drive efficiency (in A/W) decreases from 0.0156 in the reference to 0.014 for the self-consistent runs, and the normalized current drive efficiency ($\zeta_{(CD)}$ [10] drops from 0.34 to 0.31. The time evolution of these quantities is shown in figure 10.

3.3. Self-consistent time evolution of plasma parameters and safety factor

The figure 10 shows the time evolution of key plasma parameters, such as average temperature, average density, total current (I_{total}), EC-driven current (I_{EC}), normalized beta (β_N), and the Greenwald density fraction. These parameters are tracked as the prescribed ECCD profile is replaced with a self-consistently

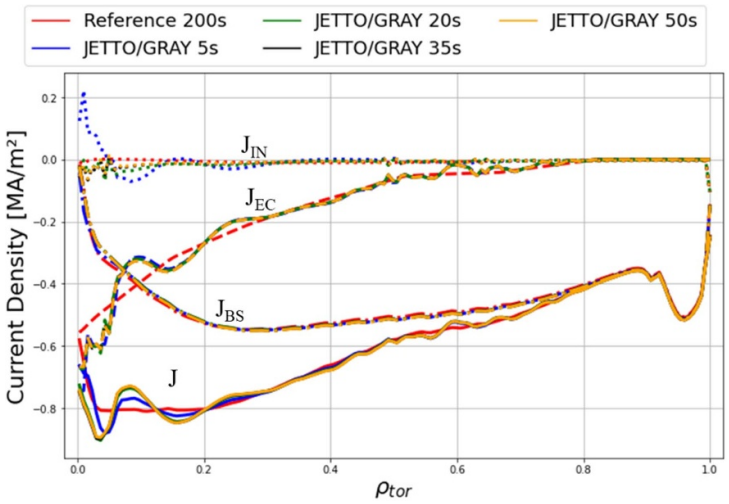

Figure 8. Shows the total current density (J) and its contributions from bootstrap (J_{BS}), electron cyclotron (J_{EC}), and inductive (J_{IN}) contributions for the self-consistent simulations at different time intervals, compared to the reference steady-state run.

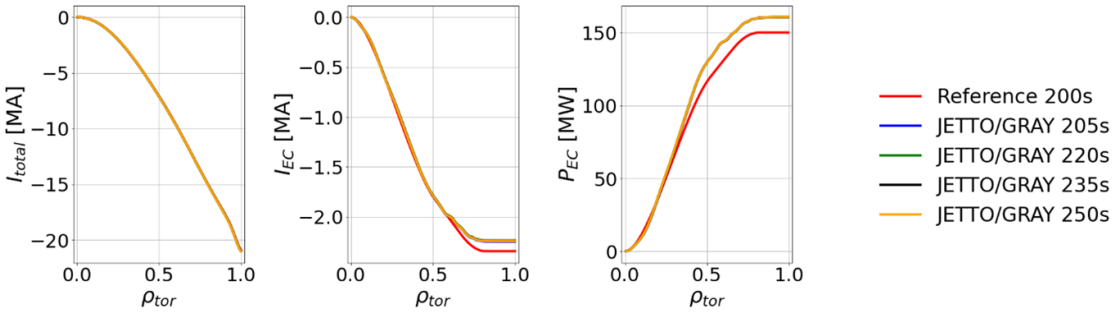

Figure 9. Radial profiles of integral quantities within the flux surface—total current (I_{total}), EC-driven current (I_{EC}), and EC power injected (P_{EC}) for self-consistent simulations at various time intervals.

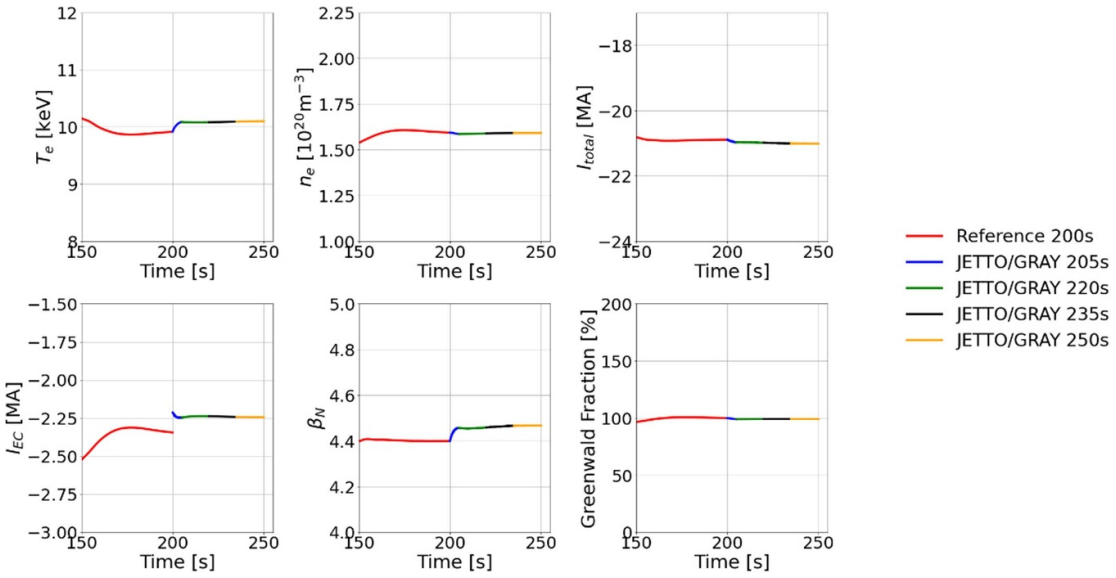

Figure 10. Evolution of plasma parameters such as temperature, $<T_e>$, density $<n_e>$, total current (I_{total}), EC driven current (I_{EC}), normalized beta (β_N) and Greenwald fraction for JETTO/GRAY self-consistent from end of reference run at 200 s to 250 s.

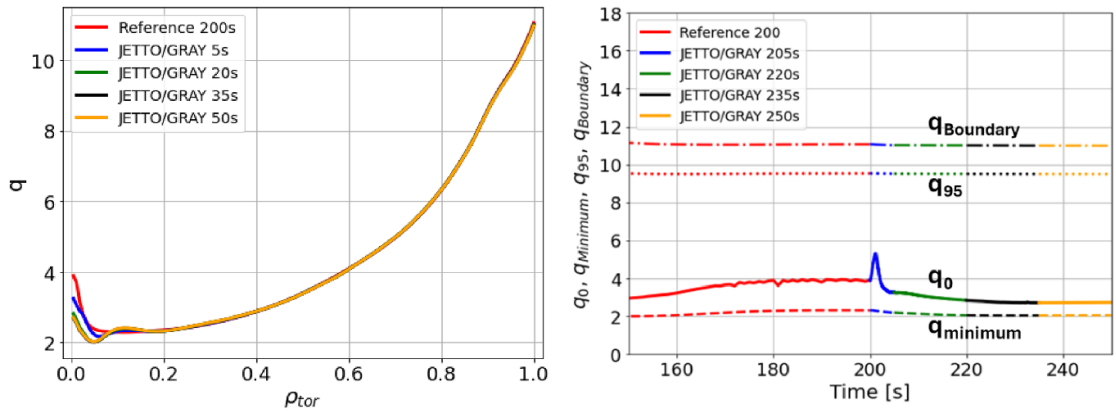

Figure 11. Q profile at the end of each reference (left) and JETTO/GRAY coupled self-consistent simulations; q_0, $q_{\min}$, q_{95} and q_{Boundary} evolution with time (right).

evolving EC-heated current drive profile. The red curve, spanning 0–200 s (plotted for 150–200 s), represents the reference steady-state run, which had already reached equilibrium at 200 s. Subsequent runs extending beyond this time show evolution of the JETTO/GRAY coupled self-consistent modeling from the reference case.

The difference in EC current and β_{N} arises due to the difference in injected EC power of 160 MW in the self-consistent simulation versus 150 MW in the reference case. When the prescribed analytic ECCD profile is replaced with the launcher-resolved profiles at 200 s, a transient adjustment occurs due to the induced back EMF, which modifies the inductive current component. This leads to a small but distinct change in the central safety factor (q^0) and an associated rise in β_{N}, as the plasma redistributes current to maintain magnetic equilibrium. Despite this, the self-consistent run exhibits only minor variations, with temperature and density changes of approximately ∼1.9% and ∼0.45%, respectively.

Figure 11 (left) shows the safety factor profile at the core (q_0) at the end of each run. The profiles align well across most of the plasma ($0.1 < \rho < 1$), with differences mainly observed in the core region. Specifically, the reversed sheer q_0 in the reference steady-state run (red curves) drops to a lower value in the later JETTO/GRAY coupled self-consistent simulations. However, the overall q profile shape remains largely unchanged.

Examining the time evolution of q_0, $q_{\min}$, q_{95}, and q_{Boundary} (figure 11, right), q_0 decreases by about 30% at the end of the JETTO/GRAY coupled self-consistent simulation compared to the reference run, while $q_{\min}$ exhibits a smaller reduction over the same period. During the self-consistent phase from 215 s to 250 s, both q^0 and $q_{\min}$ remain nearly constant, indicating that the system has reached a quasi-steady state. In contrast, q_{95} and q_{Boundary} show negligible variation throughout the final 50 s of the run with the realistic EC profile. This behavior confirms that the JETTO/GRAY coupling accurately captures the plasma's self-regulating response to the new ECCD configuration and maintains equilibrium self-consistently during the transition.

4. Summary and future work

This work presents self-consistent EC heating, transport and equilibrium modeling of the steady state scenario by replacing the prescribed ECCD with a realistic one. To that end, parametric GRAY single-ray scans were performed across an extensive range of launching parameters to determine the optimal configurations. The GRAY code was then re-run for the selected optimal launchers, with results scaled linearly to match the prescribed ECCD profile in the reference case. Once these optimized ECCD profiles were integrated into JETTO, replacing the prescribed ECCD, the JETTO/GRAY coupled simulation successfully evolved over 50 s, demonstrating the feasibility of a self-consistent plasma evolution.

The self-consistent simulation exhibited only minor deviations from the reference plasma, with variations of approximately 1.9% in $<T_{\text{e}}>$ and 0.45% in $<n_{\text{e}}>$. The inductive current evolved to compensate for differences in the ECCD profile at the start of the JETTO/GRAY runs but stabilized towards the end of the 50 s self-consistent simulation. The reference steady-state scenario with prescribed ECCD was modeled with 150 MW of EC input power, while in the self-consistent JETTO/GRAY run at 250 s, the input power was set to 160 MW. The global current drive efficiency (in A/W) shows a slight reduction from 0.0156 to 0.014, and the normalized current drive efficiency (ζ_{CD}) drops from 0.34 to 0.31.

Additionally, the q-profiles remain largely unchanged in the final self-consistent runs. However, $q_{\min}$ falls below the desirable threshold of 2.3, indicating that maintaining it above this limit will require further refinement in future work.

The primary objective of this study was to demonstrate the feasibility of running JETTO coupled with GRAY using a realistic current drive model, based on a steady-state flat-top scenario [5] with a simple transport model and interpretive impurity treatment. This study provides a methodology for achieving this, which can be applied to future STEP scenarios. For future work, several extensions and improvements are planned. One key area is the inclusion of realistic impurity profiles and variable *Zeff*, as current simulations assume a constant flat *Zeff* profile. Accounting for impurity fluctuations will allow for more accurate predictions of ECCD performance. In addition, focus will be on incorporating more sophisticated transport models with predictive confinement capability.

As the STEP HCD design evolves, launcher geometries will change. Updated GRAY scans will be necessary to reflect these modifications and maintain ECCD efficiency, ensuring that the optimized ECCD profiles remain valid as the design progresses.

Although an extensive parameter space was explored during the optimization process, the final launcher configuration will ultimately require simplification—particularly regarding the number of operating frequencies and power limitations per launcher. Future developments will also involve the implementation of EC controllers that dynamically adjust the EC system to achieve the desired current profile in an evolving plasma.

Finally, while this study focuses on the steady-state phase, future research will extend the methodology to include the ramp-up and ramp-down phases. These transient periods introduce distinct challenges for ECCD optimization. In particular, the bootstrap current is either significantly reduced or absent, requiring the ECCD system to compensate by driving a larger fraction of the total plasma current. This increases the demand on the HCD system in terms of both power and efficiency. Additionally, the evolving plasma density and temperature profiles during these phases can alter the accessibility and effectiveness of different launchers. This necessitates dynamic adjustment of launcher parameters to maintain reliable current drive and heating performance throughout the entire operational cycle of the STEP power plant.

Data availability statement

All data that support the findings of this study are included within the article (and any supplementary files).

Error Analysis available at https://doi.org/10.1088/1361-6587/ae2a6b/data1.

Acknowledgment

This work has been funded by STEP, a UKAEA programme to design and build a prototype fusion energy plant and a path to commercial fusion. To obtain further information on the data and models underlying this paper please contact PublicationsManager@ukaea.uk.

Author contributions

R Sharma 0000-0002-2804-086X

Supervision (lead), Validation (lead), Visualization (lead), Writing – original draft (lead), Writing – review & editing (lead)

Appendix. Simdb catalogue modeling runs

Time (s)	Simdb reference	UUID
0–200	kkirov/jetto/step/88 888/aug2322/seq-1	8cf32704239711ed855ed36d00883459
200–201	sharmar/jetto/step/88 888/mar2823/seq-2	91 c306e0-d3c9-11ed-b93d-d1feb20c989b
200–205	sharmar/jetto/step/88 888/apr1123/seq-1	5d191c44dd1b11ed87e82b08cc75d417
205–220	sharmar/jetto/step/88 888/aug1423/seq-1	03e9f822-03 da-11f0-b109-33ea76003e10
220–235	sharmar/jetto/step/88 888/aug2223/seq-1	4e923d40-03de-11f0-922 c-0512d8c71e9d
235–250	sharmar/jetto/step/88 888/aug2423/seq-1	fced0d1c-03e2-11f0-97f0-61eec2bf80c1

References

[1] Henderson M *et al* 2023 The concept design of the STEP heating and current drive system *29th IAEA Fusion Energy Conf.* (*London, United Kingdom*)

[2] Freethy S, Figini L, Craig S, Henderson M, Sharma R and Wilson T 2024 The optimisation of the STEP electron cyclotron current drive concept *Nucl. Fusion* **64** 126035

[3] Romanelli M *et al* 2014 JINTRAC: a system of codes for integrated simulation of tokamak scenarios *Plasma Fusion Res.* **9** 3403023

[4] Poli E, Tardini G, Zohm H, Fable E, Farina D, Figini L, Marushchenko N B and Porte L 2013 Electron cyclotron heating and current drive with GRAY and JETTO: integration for self-consistent tokamak modelling *Nucl. Fusion* **53** 013011

[5] Tholerus E *et al* 2024 Flat-top plasma operational space of the STEP power plant *Nucl. Fusion* **64** 106030

[6] Farina D 2007 Ray tracing and quasi-optical methods for electron cyclotron absorption and current drive *Fusion Sci. Technol.* **52** 154–60

[7] Fisch N J 1987 Theory of current drive in plasmas *Rev. Mod. Phys.* **59** 175–234

[8] Lin-Liu Y R, Chan V S and Prater R 2003 Electron cyclotron current drive efficiency in general tokamak geometry *Phys. Plasmas* **10** 4064–71

[9] Marushchenko N B, Beidler C D, Kasilov S V, Kernbichler W, Maaßberg H, Prater R and Harvey R W 2011 Electron cyclotron current drive in low collisionality limit: on parallel momentum conservation *Phys. Plasmas* **18** 032501

[10] Luce T C, Lin-Liu Y R, Harvey R W, Giruzzi G, Politzer P A, Rice B W, Lohr J M, Petty C C and Prater R 1999 Generation of localized noninductive current by electron cyclotron waves on the DIII-D Tokamak *Phys. Rev. Lett.* **83** 4550–3